

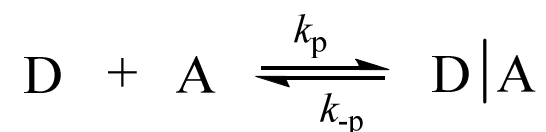
Marcus Theory of Electron Transfer

- From a molecular perspective, Marcus theory is typically applied to *outer sphere* ET between an electron donor (D) and an electron acceptor (A).
- For convenience in this discussion we will assume D and A are neutral molecules so that electrostatic forces may be ignored.
- It is also worth considering that either D or A may be in a photoexcited state (*photoinduced electron transfer aka PET*).
- Other than a change in the starting stage energies, the principles of Marcus' model apply equally well to both ground and excited state electron transfer.

For second-order reactions between a homogenous mixture of D and A the reaction can be broken down into three steps:

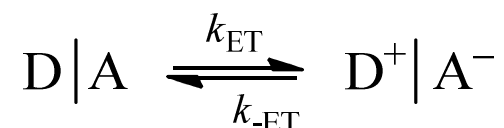
1. Precursor complex

D and A diffuse together with a rate constant k_a to form an outer sphere precursor complex D|A. Dissociation of the precursor complex without ET is described by k_d .



2. Successor complex

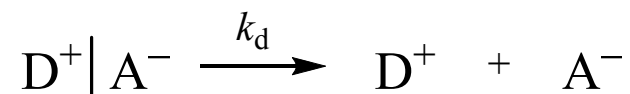
The precursor complex D|A undergoes reorganization toward a transition state in which ET takes place to form a successor complex $D^+|A^-$.

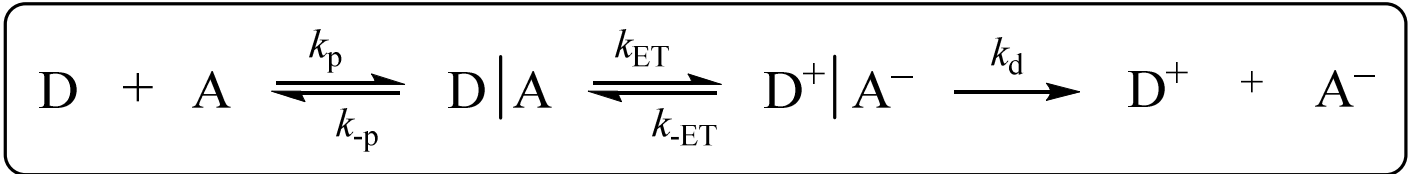


The nuclear-configuration of the precursor and successor complexes at the transition state must be identical for successor complex to form.

3. Dissociation

Finally, the successor complex dissociates forming the independent D^+ cation and A^- anion.





- Using a steady-state approximation k_{obs} can be estimated as

$$k_{obs} = \frac{k_p}{1 + \frac{k_{-p}}{k_{ET}} + \frac{k_{-p}k_{-ET}}{k_d k_{ET}}} \quad \text{eqn. 1}$$

which can be rearranged to

$$\frac{1}{k_{obs}} = \frac{1}{k_p} + \frac{k_{-p}}{k_p k_{ET}} \left[1 + \frac{k_{-ET}}{k_d} \right] \quad \text{eqn. 2}$$

- If $k_d \gg k_{-ET}$ eqn. 2 reduces to

$$\frac{1}{k_{obs}} = \frac{1}{k_p} + \frac{k_{-p}}{k_p k_{ET}} \quad \text{eqn. 3}$$

- If $k_{-p} \gg k_{ET}$ eqn. 3 reduces to

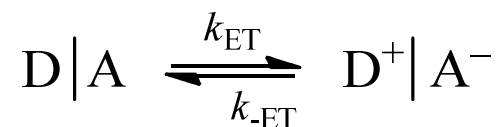
$$k_{obs} \cong \frac{k_p k_{ET}}{k_{-p}} \quad \text{eqn. 3a}$$

- Conversely, if $k_{-p} \ll k_{ET}$

$$k_{obs} \cong k_p \quad \text{eqn. 3b}$$

and the second order ET rate constant will contain no information about k_{ET}

- If D and A are covalently linked, or even fixed within a close distance (e.g. H-bonding, protein matrix) only the ET step need be considered.



k_{ET} and k_{-ET} can then, in principle at least, be directly observed.

- Knowledge of the various state energies is critical for the interpretation of kinetic data for electron transfer with Marcus theory.
- This is particularly true for PET. For example, the first singlet excited state S_1 energy may be estimated by the point of overlap for normalized absorption ($S_0 \rightarrow S_1$) and emission ($S_0 \leftarrow S_1$) bands.
- With the $S_0 \rightarrow T_1$ transition typically absent, the T_1 energy is usually estimated by the blue edge of the low-temperature phosphorescence spectrum (assuming a negligible Stokes shift between $S_0 \rightarrow T_1$ and $S_0 \leftarrow T_1$).
- The energies of D^+ and A^- can be easily obtained by electrochemical methods, e.g. linear and cyclic voltammetry, differential pulse and square wave voltammetries.

- The Gibbs energy difference under standard conditions between the “D + A” and “D⁺ + A⁻” states can be approximated as

$$\Delta G^o = e(E_{D^+/D}^o + E_{A/A^-}^o) + \omega^p - \omega^r$$

e = electronic charge

E^o = standard reduction potential

ω = work, i.e. energy used in bringing reactants (-tive) and products (-tive) together.

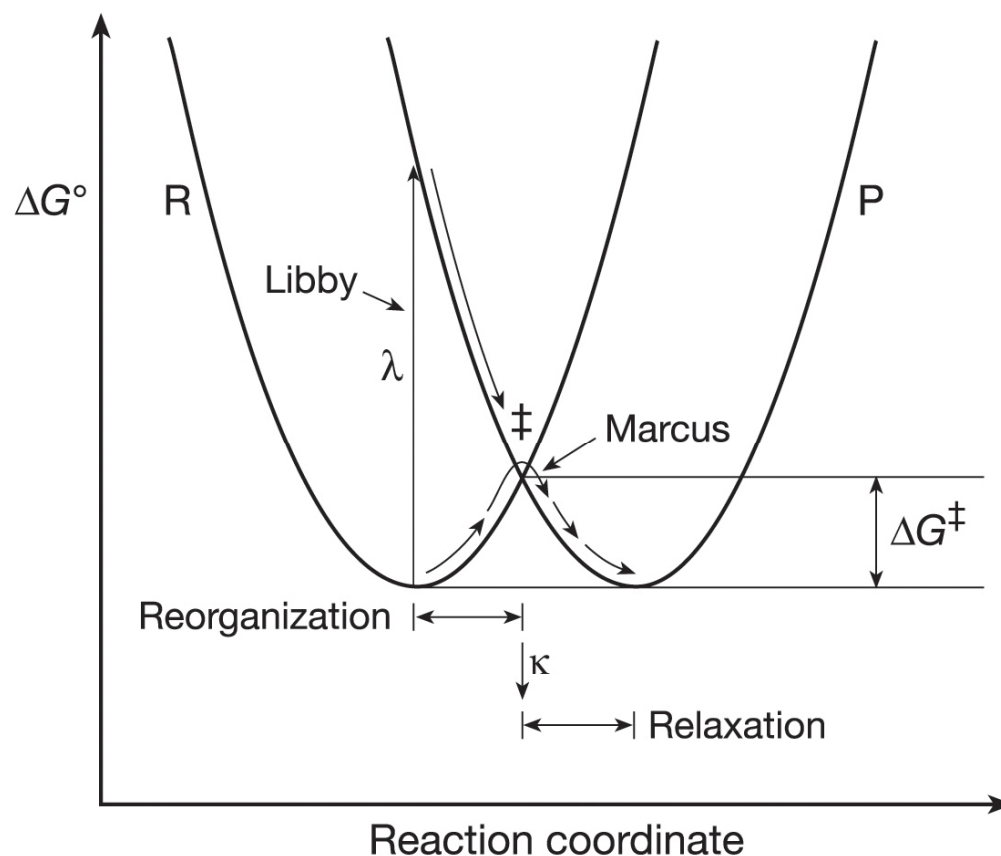
- From here on we will assume only covalently linked D-A supramolecular species where

$$\Delta G^o = e(E_{D^+/D}^o + E_{A/A^-}^o)$$

- The potential energies of ground, excited, transition and product states are all dependent upon the many nuclear coordinates involved inclusive of the solvation cage and its associated energies.
- In transition state theory a *reaction coordinate* is introduced so that the potential energy surface can be reduced to a one-dimensional profile.

- Curve R represents the reactant state $D|A$ while curve P represents the product state $D^+|A^-$
- For ET to occur the reactant state must distort from its equilibrium energy state to reach a transition state geometry \ddagger which also exists as a distorted form of the product state.
- Electron transfer occurs at the point along the reaction coordinate as the transition state has a 50% probability of producing the $D^+|A^-$ product state (at least in this ideal symmetrical case with $\Delta G^\circ = 0$)

[note: Marcus theory assumes R and P curves are of equal shape. This model neglects external solvation effects, when included give a more accurate non-parabolic picture]



$$\Delta G^\ddagger = \frac{(\lambda + \Delta G^\circ)^2}{4\lambda}$$

- According to classical transition state theory

$$k_{\text{ET}} = \kappa_{\text{el}} \nu_{\text{n}} \exp\left(\frac{-\Delta G^{\ddagger}}{k_{\text{B}} T}\right)$$

κ_{el} = electron transmission coefficient (~ 1)

ν_{n} = vibrational frequency of the transition state (D | A) ‡ ($\sim 10^{13} \text{ s}^{-1}$)

k_{B} = Boltzmann constant

T = temperature (K)

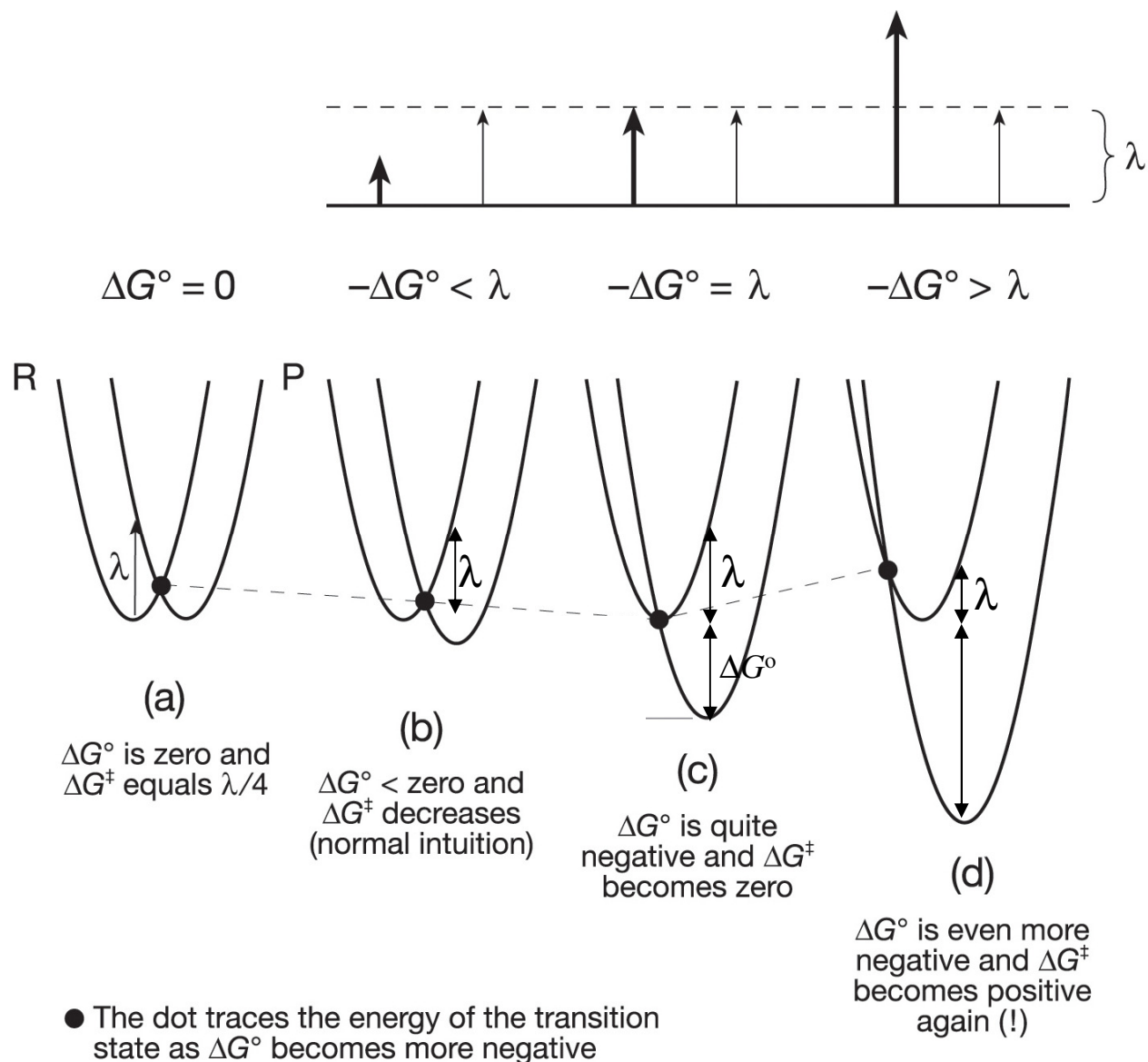
ΔG^{\ddagger} = Gibbs free energy of activation

- Thus, following the mathematical description of parabolic curves where

$$\Delta G^{\ddagger} = \frac{(\lambda + \Delta G^{\circ})^2}{4\lambda}$$

the classical Marcus equation can be written as:

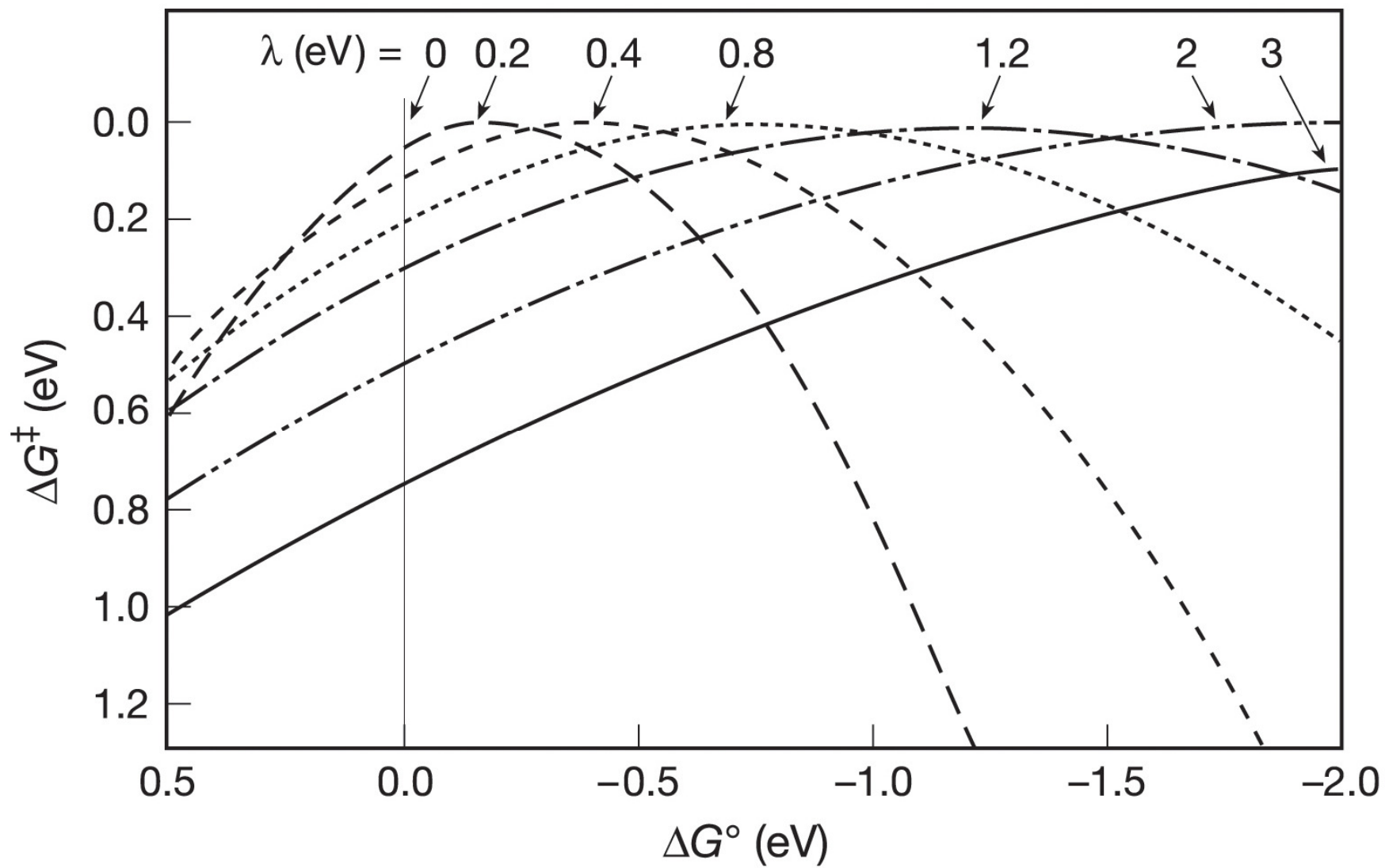
$$k_{\text{ET}} = \kappa_{\text{el}} \nu_{\text{n}} \exp\left[\frac{-(\lambda + \Delta G^{\circ})^2}{4\lambda k_{\text{B}} T}\right]$$



The **reorganization energy** (λ) is defined as the change in Gibbs energy if the reactant state ($D | A$) were to distort to the equilibrium conformation of the product state ($D^+ | A^-$) without transfer of an electron.

$$k_{\text{ET}} = \kappa_{\text{el}} v_{\text{n}} \exp \left[\frac{-(\lambda + \Delta G^{\circ})^2}{4\lambda k_{\text{B}} T} \right]$$

- The Marcus equation implies that for moderately exergonic reactions ΔG^{\ddagger} will decrease while k_{ET} will increase as ΔG° becomes more negative.
- When $\Delta G^{\ddagger} = 0$ and $-\Delta G^{\circ} = \lambda$, k_{ET} reaches its maximum value of $\kappa_{\text{el}} v_{\text{n}}$
- However, as $-\Delta G^{\circ}$ becomes more negative in a highly exergonic reaction, the intersection point of R and P surfaces moves to the left causing ΔG^{\ddagger} to increase again realizing that k_{ET} will actually begin to decrease as the reaction becomes highly exergonic.
- This “contradictory” observation is known as the **Marcus inverted region**.



Adiabatic vs. non-adiabatic electron transfer

- Two types of electron transfer reactions can be distinguished according to the magnitude of the *electronic coupling factor* H_{rp} between the reactant and product states.

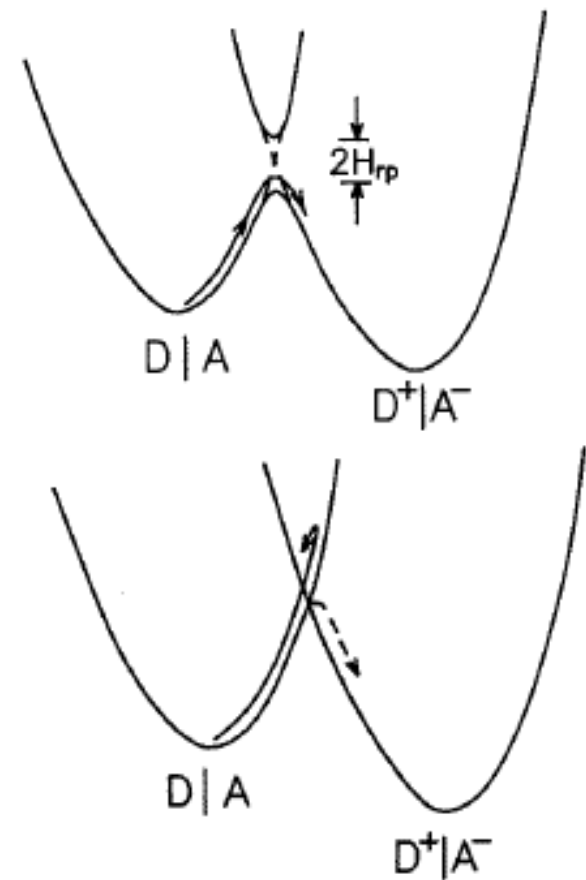
$$H_{rp} = \langle \psi_r^0 | \mathcal{H}_{el} | \psi_p^0 \rangle$$

ψ^0 = electronic wavefunction for reactant and product states

\mathcal{H}_{el} = the Born-Oppenheimer electronic Hamiltonian for the system.

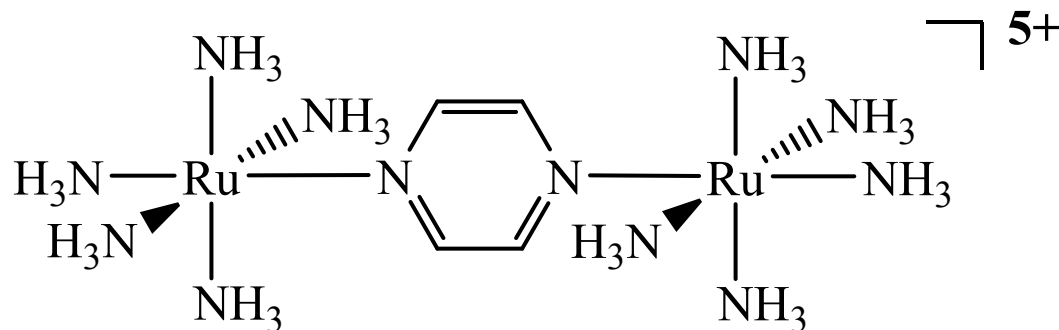
- **Large H_{rp} = adiabatic ($\kappa_{el} \sim 1$)**
- **Small H_{rp} = non-adiabatic ($\kappa_{el} \ll 1$)**

- For transition metal redox reactions the point of demarcation between adiabatic and non-adiabatic is where $H_{rp} \sim 0.025$ eV.
- H_{rp} decreases exponentially with distance between D and A



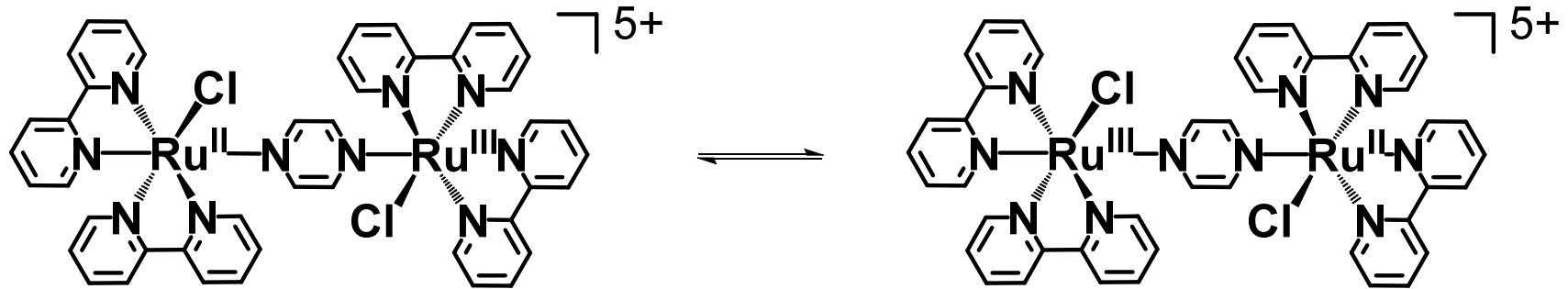
Mixed valence transition metal complexes

- Mixed-valence compounds contain an element which, at least in a formal sense, exists in more than one oxidation state.
- This is a common phenomenon, e.g. Prussian blue which has a cyanide-bridged Fe(II)-Fe(III) structure, was one of the first chemical materials to be described.
- In the 1970s the first designed mixed-valence complexes were prepared, the μ -pyrazine-bridged dimer $[(\text{NH}_3)_5\text{Ru}(\text{pz})\text{Ru}(\text{NH}_3)_5]^{5+}$ by Carol Creutz and Henry Taube.



- One of the reasons for interest in mixed-valence molecules was the possibility that they could be used to measure rate constants and activation barriers for intramolecular electron transfer

- These reactions have proven difficult to study by direct measurement, but the analogous light-driven process can often be observed as a broad, solvent-dependent absorption band.
- For symmetrical mixed-valence complexes these bands typically appear in low-energy visible or near-infrared spectra.
- They are typically called intervalence transfer (IT), metal-metal charge transfer (MMCT), or intervalence charge transfer (IVCT) bands.
- Hush provided an analysis of IT band shapes based on parameters that also define the electron-transfer barrier.
- The barrier arises from nuclear motions whose equilibrium displacements are affected by the difference in electron content between oxidation states.
- This includes both intramolecular structural changes and the solvent where there are changes in the orientations of local solvent dipoles.



- In the above example, the geometrical distance between the metal centers (6.9 Å) is sufficiently large that direct overlap of the electronic wave functions is negligible.
- Electronic coupling occurs indirectly by mixing of metal-based donor and acceptor orbitals of appropriate symmetry in the bridge.
- The electronic coupling matrix element arising from donor-acceptor coupling is often called H_{ab} (as reactant is indistinguishable from the product state)
- As H_{ab} increases, the discrete oxidation-state character of the local sites decreases and with it structural differences and dipole orientational changes in the solvent.
- It also mixes the donor and acceptor orbitals along the ligand bridge or organic spacer, which has the effect of decreasing the electron transfer distance.

- A linear combination of the initial, zero-order, diabatic (noninteracting) wave functions for the electron transfer reactants [Ψ_a for Ru(III)-Ru(II)] and products [Ψ_b for Ru(II)-Ru(III)], including the interaction between them, gives rise to two new adiabatic states of energies E_1 and E_2 .
- The associated wave functions, Ψ_1 and Ψ_2 , are linear combinations of Ψ_a and Ψ_b .
- Energies of the unperturbed initial and final diabatic states are described by

$$H_{aa} = \langle \Psi_a | \mathcal{H}_{el} | \Psi_a \rangle \qquad H_{bb} = \langle \Psi_b | \mathcal{H}_{el} | \Psi_b \rangle$$

- Mixing between states is described by the electronic coupling matrix element

$$H_{ab} = \langle \Psi_a | \mathcal{H}_{el} | \Psi_b \rangle$$

$$E_1 = \frac{(H_{aa} + H_{bb})}{2} - \frac{[(H_{aa} - H_{bb})^2 + 4H_{ab}^2]^{1/2}}{2}$$

$$E_2 = \frac{(H_{aa} + H_{bb})}{2} + \frac{[(H_{aa} - H_{bb})^2 + 4H_{ab}^2]^{1/2}}{2}$$

- These expressions assume a symmetrical mixed-valence molecule with zero driving force for electron transfer.

$$\Delta G^o = 0 (H_{aa}^o = H_{bb}^o)$$

- The coordinate x , is the displacement from the energy minimum at $x = 0$.
- The displacement difference between the minima before and after electron transfer is a . The corresponding energies at the minima are H_{aa}^o and H_{bb}^o .
- Equal force constants (f) are assumed for the electron transfer reactants and products. The following equations describe an average of the coupled vibrational and solvent modes assumed to be harmonic.
- When a coupled nuclear motion is included as an harmonic oscillator, H_{aa} and H_{bb} vary with the coordinate for this motion

$$H_{aa} = H_{aa}^o + fx^2/2$$

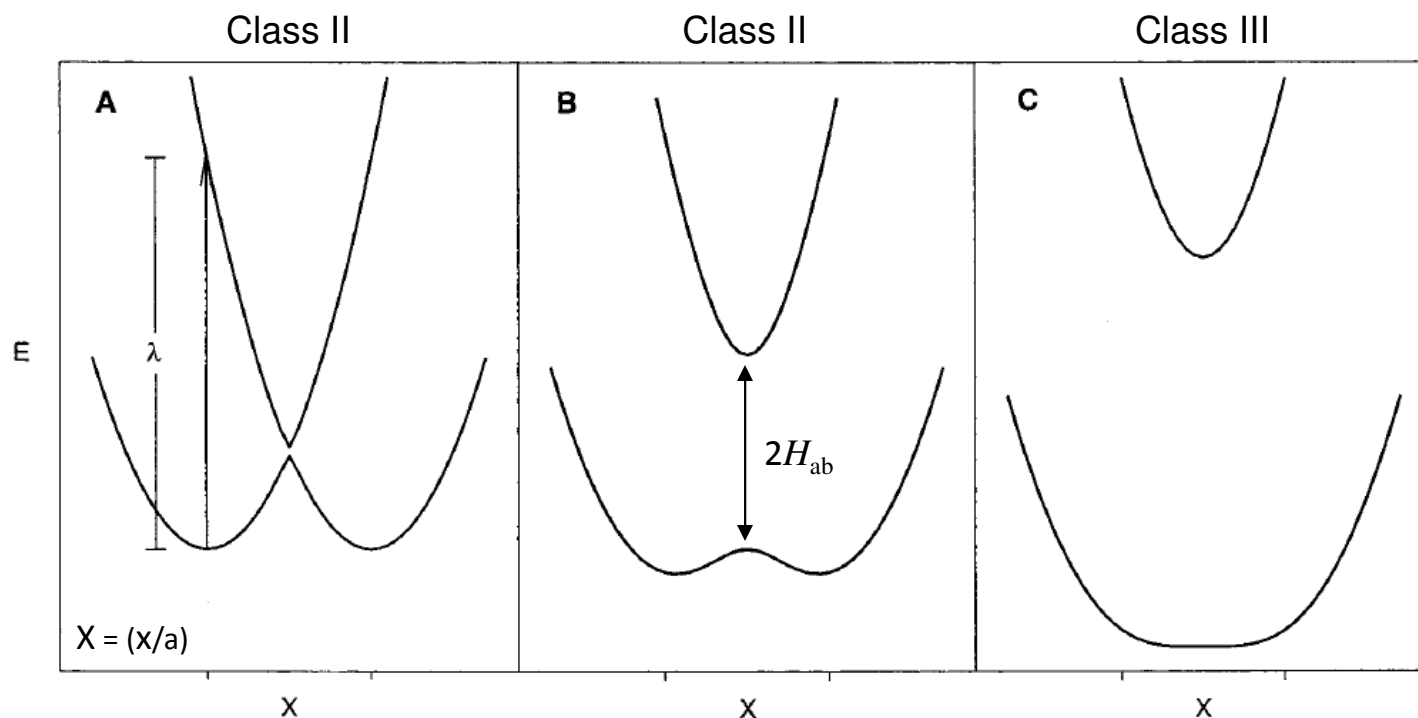
$$H_{bb} = H_{bb}^o + f(x - a)^2/2$$

- With the dependence of H_{aa} and H_{bb} on x included, the potential energy curves E_1 and E_2 are generated.

$$E_1 = \frac{\lambda(2X^2 - 2X + 1)}{2} - \frac{\{[\lambda(2X - 1)]^2 + 4H_{ab}^2\}^{1/2}}{2}$$

$$E_2 = \frac{\lambda(2X^2 - 2X + 1)}{2} + \frac{\{[\lambda(2X - 1)]^2 + 4H_{ab}^2\}^{1/2}}{2}$$

- E_1 and E_2 describe how the energies of the ground and excited state vary with the reduced nuclear coordinate $X = (x/a)$ where $\lambda = f a^2/2$.
- Depending upon the magnitude of H_{ab} supramolecular systems are typically classified according to the Robin and Day scheme, i.e. Class I, II or III systems.



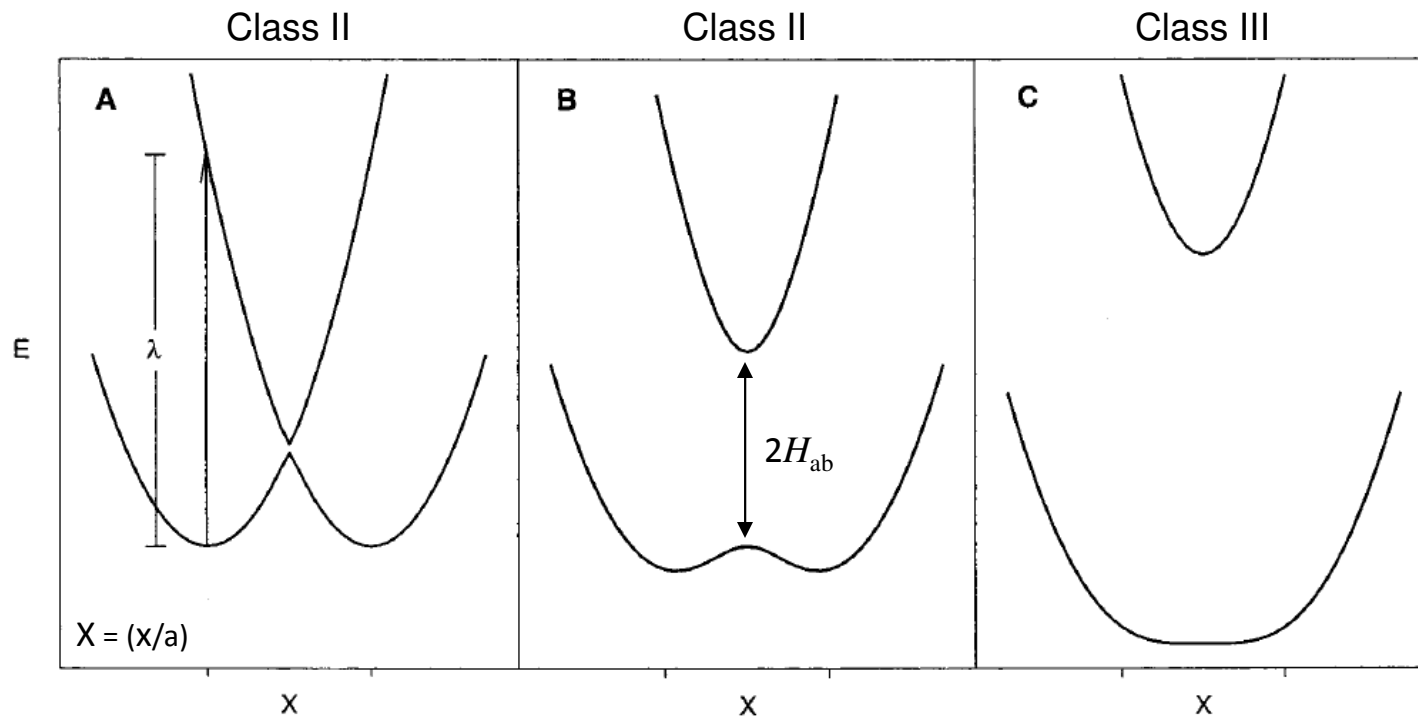
Energy-coordinate diagrams for E_1 and E_2 calculated using the following eqns.

$$E_1 = \frac{\lambda(2X^2 - 2X + 1)}{2} - \frac{\{[\lambda(2X - 1)]^2 + 4H_{ab}^2\}^{1/2}}{2}$$

$$E_2 = \frac{\lambda(2X^2 - 2X + 1)}{2} + \frac{\{[\lambda(2X - 1)]^2 + 4H_{ab}^2\}^{1/2}}{2}$$

Where $\lambda = 8000 \text{ cm}^{-1}$ (all cases) and (A) $H_{ab} = 100 \text{ cm}^{-1}$ (B) $H_{ab} = 2000 \text{ cm}^{-1}$ (C) $H_{ab} = 4000 \text{ cm}^{-1}$.

The coordinate axis is the reduced coordinate $X = (x/a)$



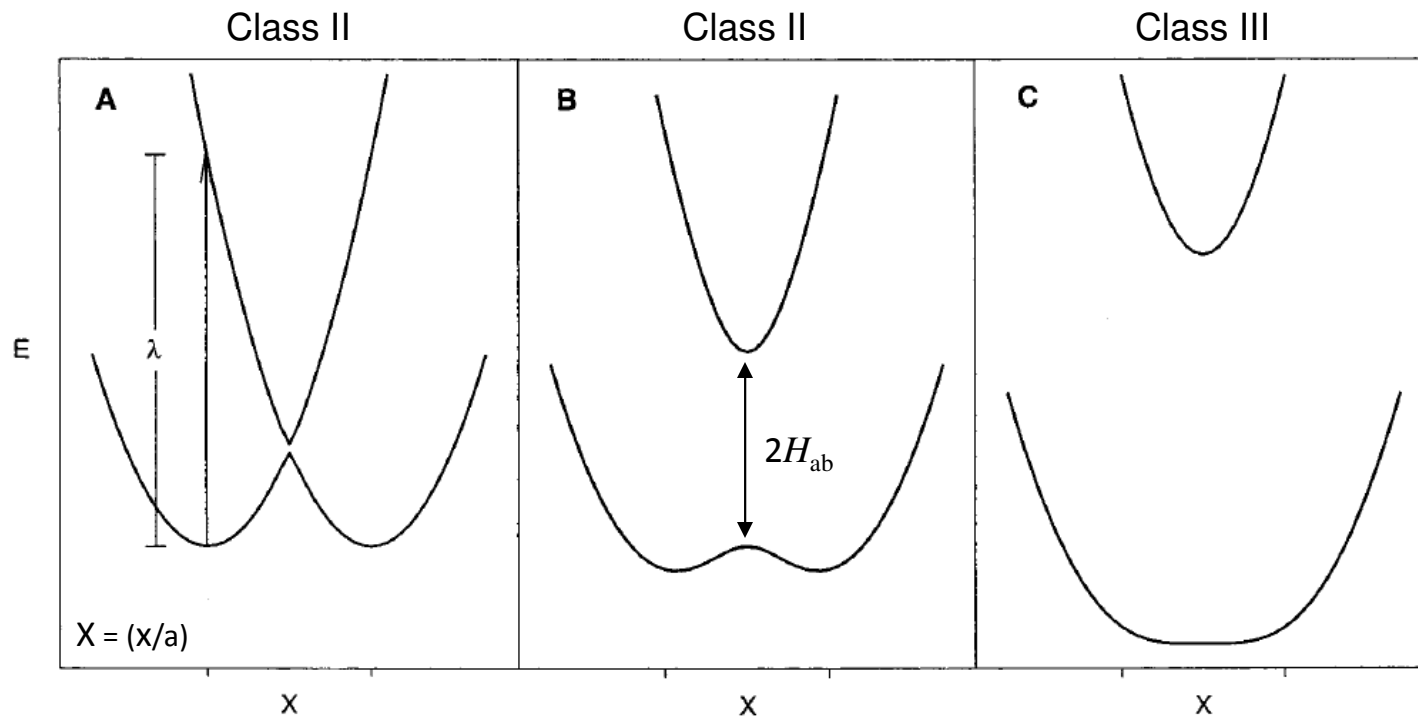
A - When $H_{ab} = 0$ both minima in the energy coordinate curve occur at $X_{\min} = 0$ and $X_{\min} = 0$.

B and **C** - With electronic coupling, the minima occur at $E_{\min} = \frac{-H_{ab}^2}{\lambda}$

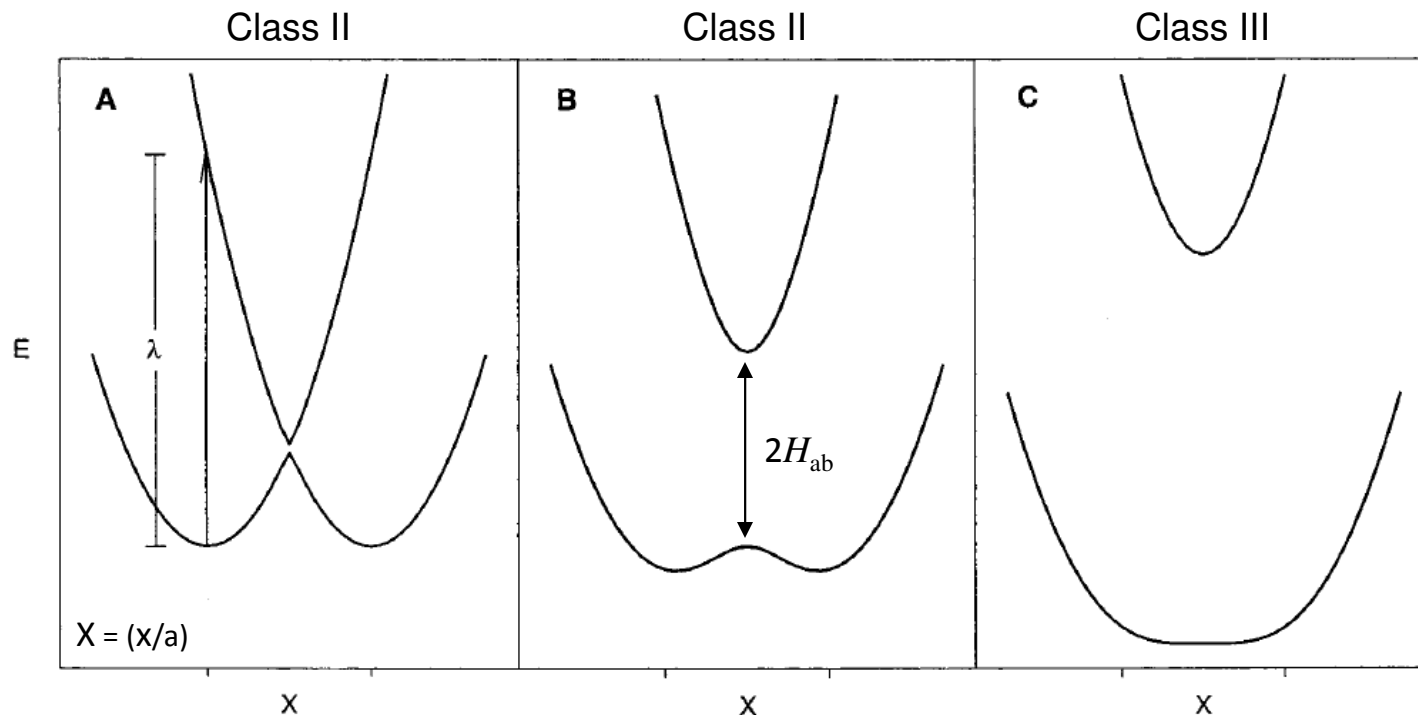
where $X_{\min} = \left\{ 1 \pm \left(1 - (4H_{ab}^2/\lambda^2) \right) \right\}^{1/2} / 2$

and the vertical difference between minima in **A** and **B** is

$$E_2 - E_1 = \left\{ [\lambda(2X - 1)]^2 + 4H_{ab}^2 \right\}^{1/2}$$



- The intervalence transfer absorption maximum corresponds to the vertical transition at X_{\min} with $E_{IT} = \lambda$ if $H_{ab} = 0$.
- In the classical limit with $H_{ab} \ll \lambda$ there is a Gaussian distribution of energies in the ground-state centered at $X = 0$ which varies with x as $\exp(-fx^2/2k_B T)$ resulting in a nearly Gaussian shaped absorption band with a maximum at $X = 0$ and $E_{IT} = \lambda = fa^2/2$



- Expressions for the absorption band maximum E_{IT} and bandwidth $\Delta\bar{\nu}_{IT}$ are

$$E_{IT} = \lambda \quad (\Delta\bar{\nu}_{IT})^2 = 16k_B T \lambda \ln 2$$

- At the top of the activation energy barrier $x = a/2$ ($X = 1/2$) $E_{IT} = \lambda/4 - |H_{ab}|$
- The energy difference from the minimum, $E_{min} = -(H_{ab}^2/\lambda)$, then gives the classical energy of activation term

$$E_a = (\lambda/4) - |H_{ab}| + (H_{ab}^2/\lambda)$$

- Expressions for the absorption band maximum E_{IT} and bandwidth $\Delta\bar{\nu}_{IT}$ are

$$E_{IT} = \lambda \text{ if } H_{ab} = 0 \qquad (\Delta\bar{\nu}_{IT})^2 = 16k_B T \lambda \ln 2$$

- At the top of the activation energy barrier $x = a/2$ ($X = 1/2$) and $E_{IT} = \lambda/4 - |H_{ab}|$
- The energy difference from the minimum, $E_{\min} = -(H_{ab}^2/\lambda)$, then gives the classical energy of activation term

$$E_a = (\lambda/4) - |H_{ab}| + (H_{ab}^2/\lambda)$$

- For a Gaussian-shaped IT absorption band, H_{ab} can be calculated from characteristic band shape parameters knowing E_{IT} and λ

$$H_{ab} (\text{cm}^{-1}) = [(4.2 \times 10^{-4}) \varepsilon \Delta\bar{\nu}_{IT} E_{IT}]^{1/2} / d$$

where ε is the molar extinction coefficient at E_{IT} and d is the e-transfer distance.

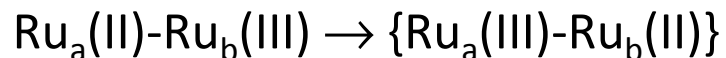
- H_{ab} is related to the absorption band regardless of shape by the relationship

$$H_{ab}^2 = [(4.2 \times 10^{-4}) E_{IT} \int \varepsilon(\bar{\nu}) d\bar{\nu}] / d^2$$

$$H_{ab} (\text{cm}^{-1}) = [(4.2 \times 10^{-4}) \varepsilon \Delta\bar{\nu}_{\text{IT}} E_{\text{IT}}]^{1/2} / d$$

- The electron transfer distance can be considerably different from the *center-to-center* distance if H_{ab} with the bridging ligand orbitals is significant.
- As such electron delocalization often results in a lower-limit for H_{ab} when the center-to-center distance is used.
- An added complication for transition metal systems is the presence of multiple IT bands. Assuming a single IT and results in an upper-limit estimate of H_{ab} . If resolved enough, the lowest energy IT band may be used to inform more accurately on H_{ab} .
- In case **B**, with H_{ab} being quantitatively significant relative to λ , and as E_{IT} approaches $k_{\text{B}}\text{T}$ ($\sim 500 \text{ cm}^{-1}$), the fraction of molecules at the top of the activation energy barrier $x = a/2$ ($X = 1/2$) $E_{\text{IT}} = \lambda/4 - |H_{ab}|$ approaches 10 %.
- Further evolution past the activation energy barrier at $x = a/2$ ($X = 1/2$) results in electron transfer and the IT band intensity should drop to zero, leading to a sharp cut off on the low-energy side of the IT absorption band.
- Spectral analysis here allows direct insight to the top of the electron transfer barrier.

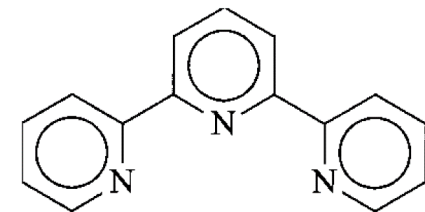
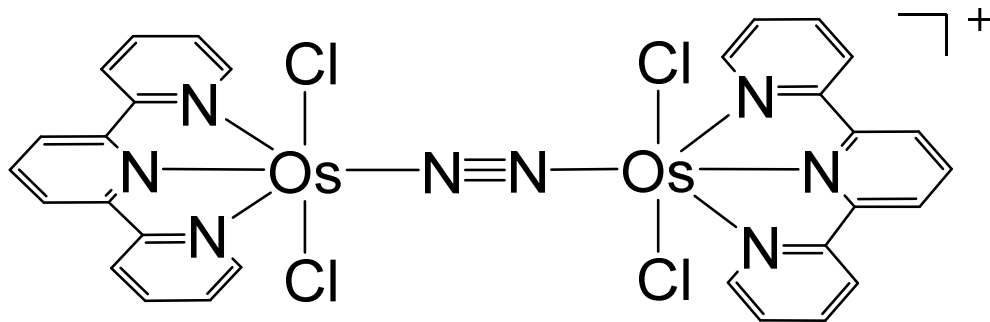
- The IT transition results in intramolecular electron transfer, e.g.,



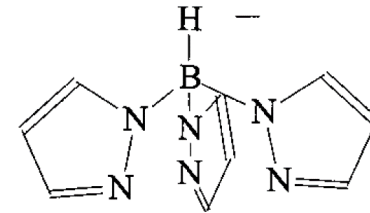
- The electron-transfer product, $\{\text{Ru}_a(\text{III})\text{-Ru}_b(\text{II})\}$, formed in excited levels of the solvent and vibrational modes coupled to the transition.
- Subsequent relaxation occurs to the intersection region at $X = 1/2$, where further relaxation or intramolecular electron transfer give a distribution of $\text{Ru}_a(\text{II})\text{-Ru}_b(\text{III})$ and $\text{Ru}_a(\text{III})\text{-Ru}_b(\text{II})$.
- In Class II there are localized valences (oxidation states) and measurable electronic coupling ($H_{ab} > 0$).
- Class I is the limiting case with $H_{ab} = 0$.
- Class III occurs when $2H_{ab}^2/\lambda \geq 1$ and there is no longer a barrier to electron transfer and the absorption band arises from a transition between delocalized electronic levels ($\Psi_a \pm \Psi_b$). Solvent coupling and λ_0 is far less than for intervalence transfer since there is no net charge transfer in the transition.

Ligand bridged Osmium complexes

- The mixed-valence N_2 bridged osmium compounds below show strong behavior characteristic of Class II complexes.

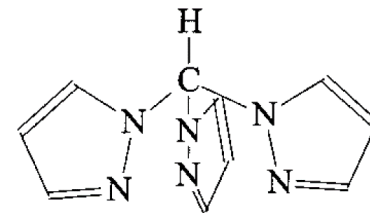


tpy

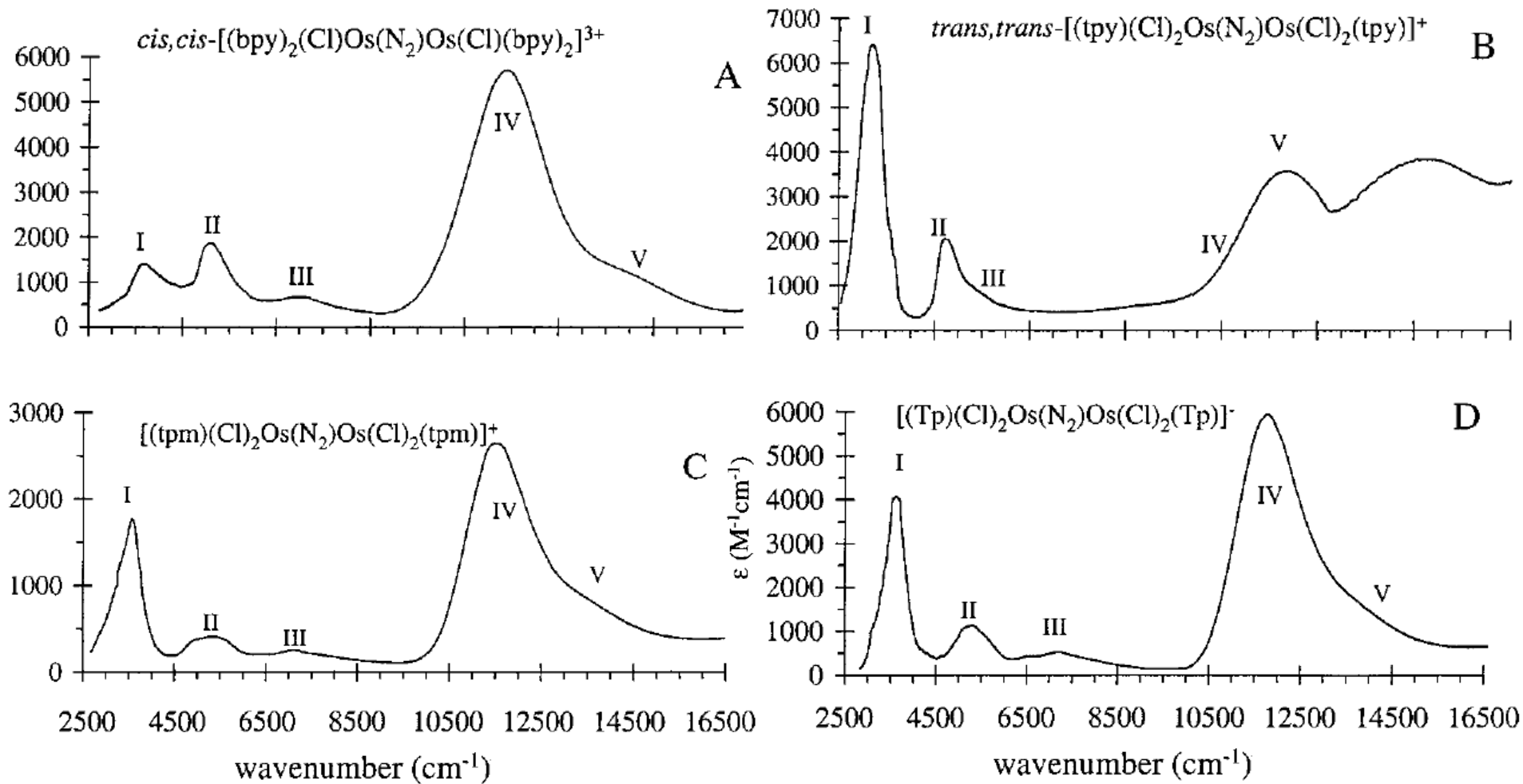


Tp

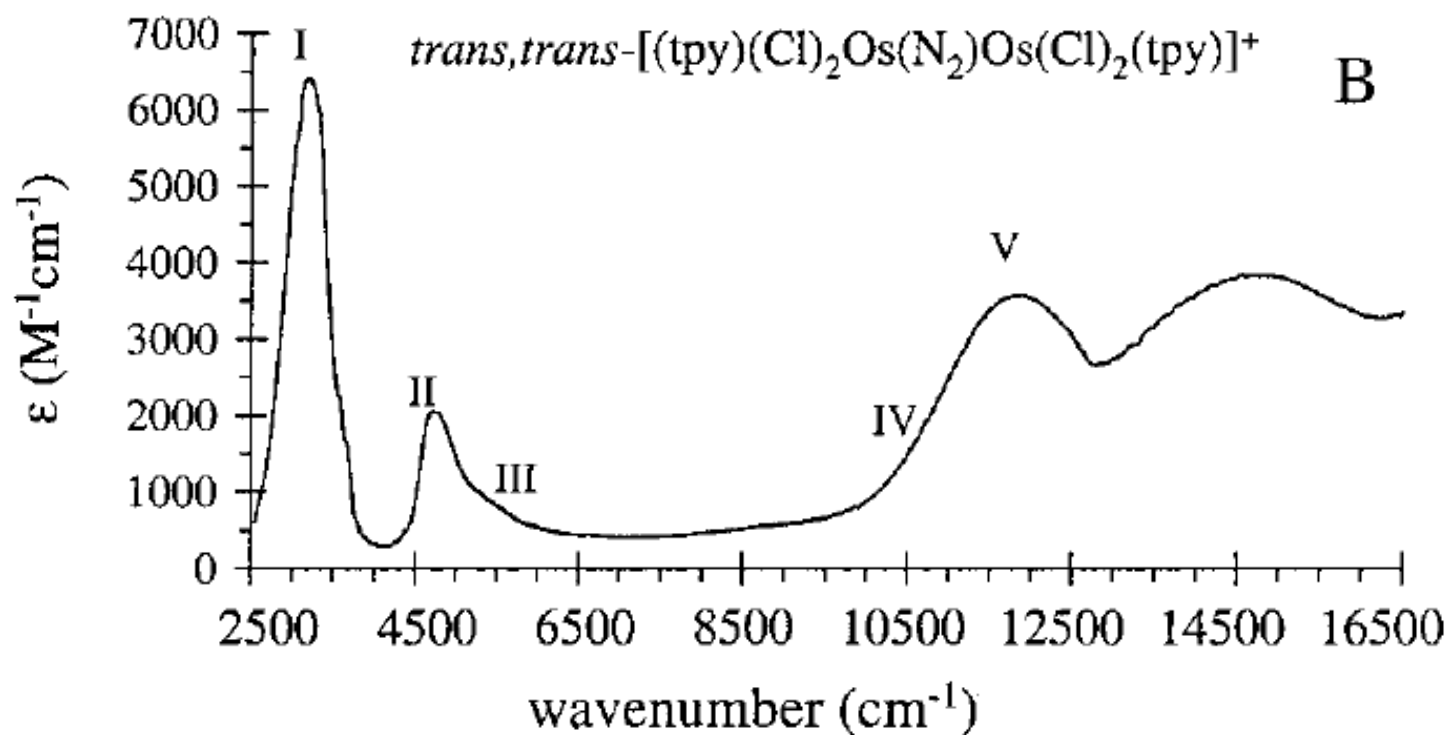
- Intense $\nu(N_2)$ stretches appear at 2007 cm^{-1} for **tpy** and 2029 cm^{-1} for **tpm** consistent with electronic asymmetry on the time scale of the IR absorption response (recorded in KBr pellets)



tpm



- IR-NIR spectra for a series of N_2 bridged mixed valence osmium complexes recorded in acetonitrile.

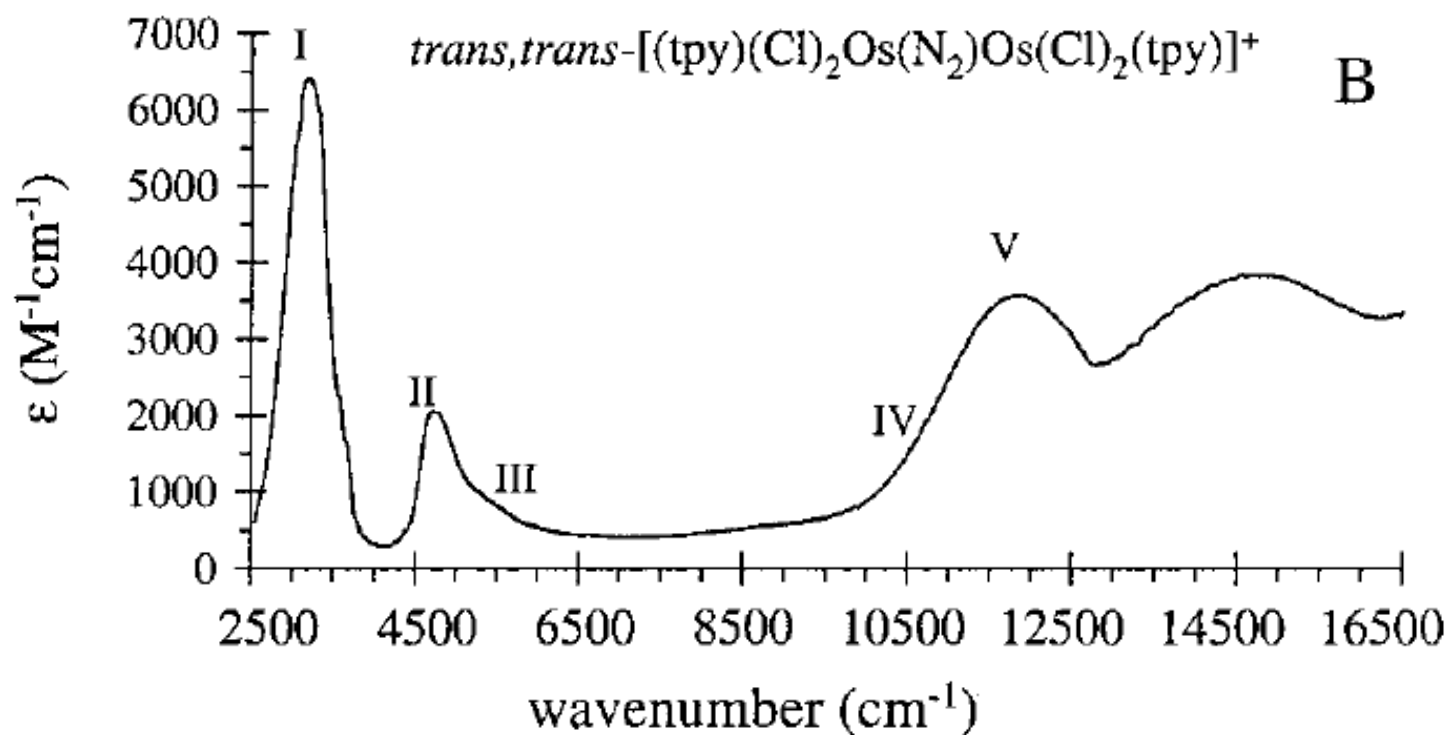


- Bands I and II provide an oxidation-state marker for Os(III).
- Due to low symmetry, extensive metal-ligand overlap, and spin-orbit coupling [$\chi = 3\,000\text{ cm}^{-1}$ for Os(III)] the d^5 Os(III) core is split into three Kramer's doublets (E'_1, E'_2, E'_3) separated by thousands of cm^{-1} .

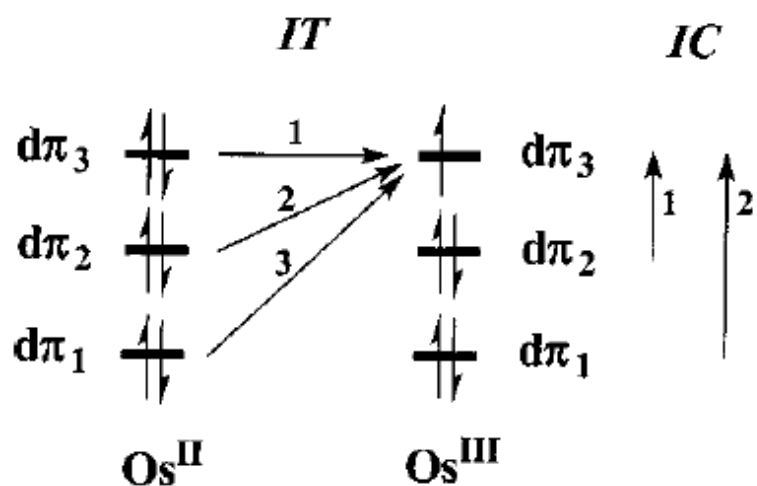
$$E'_3 = d\pi_1^1 d\pi_2^2 d\pi_3^2 \quad (\text{IC-2})$$

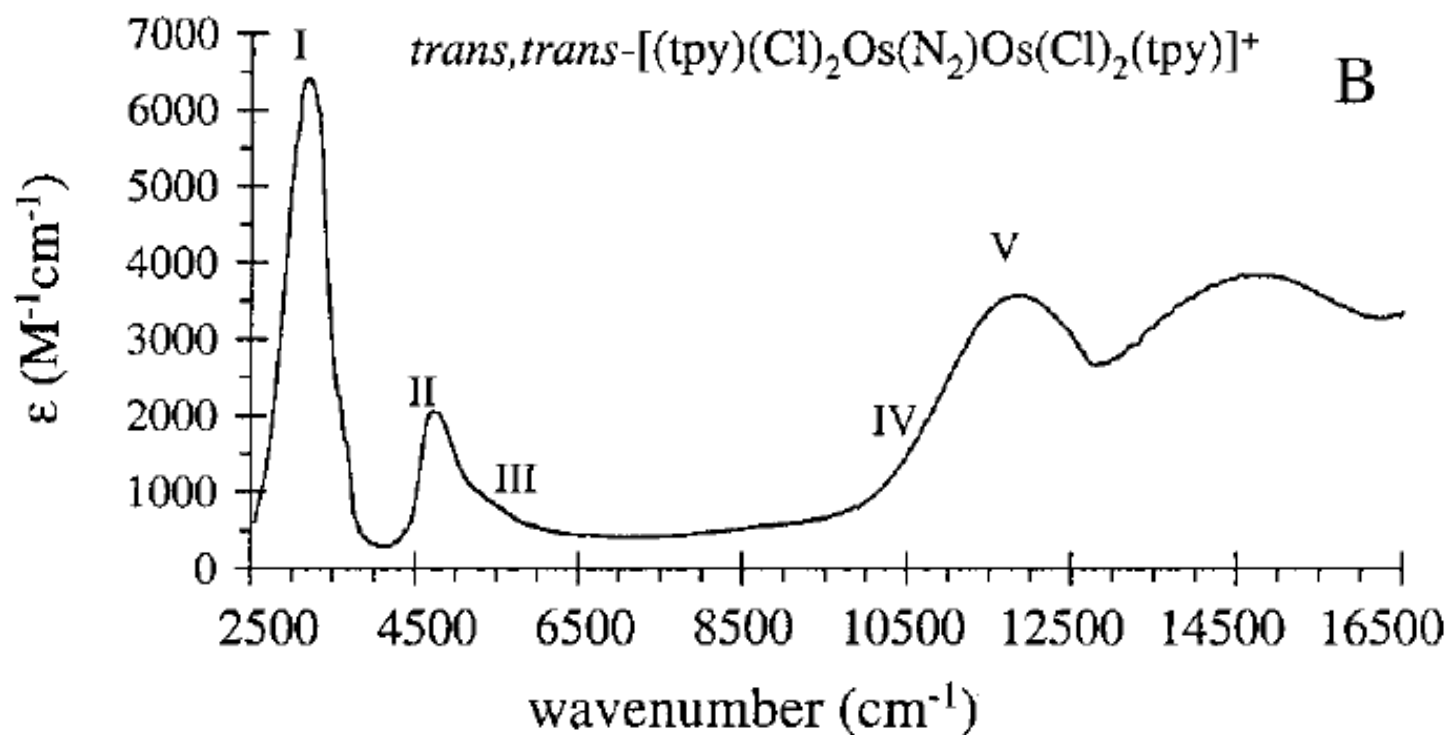
$$E'_2 = d\pi_1^2 d\pi_2^1 d\pi_3^2 \quad (\text{IC-1})$$

$$E'_1 = d\pi_1^2 d\pi_2^2 d\pi_3^1 \quad (\text{GS})$$

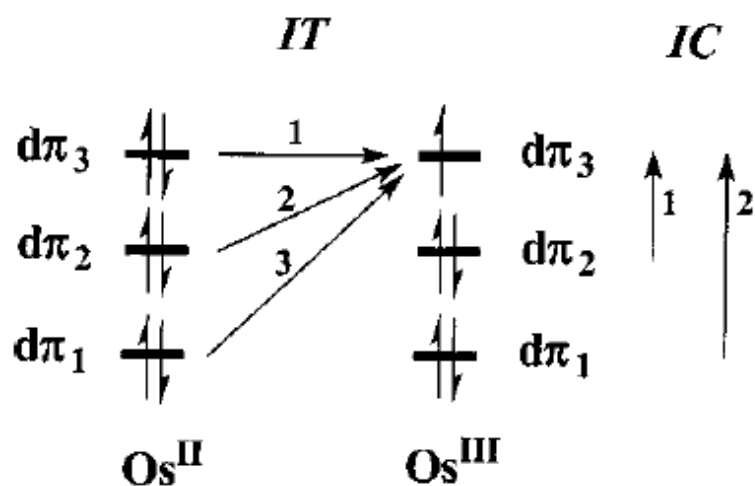


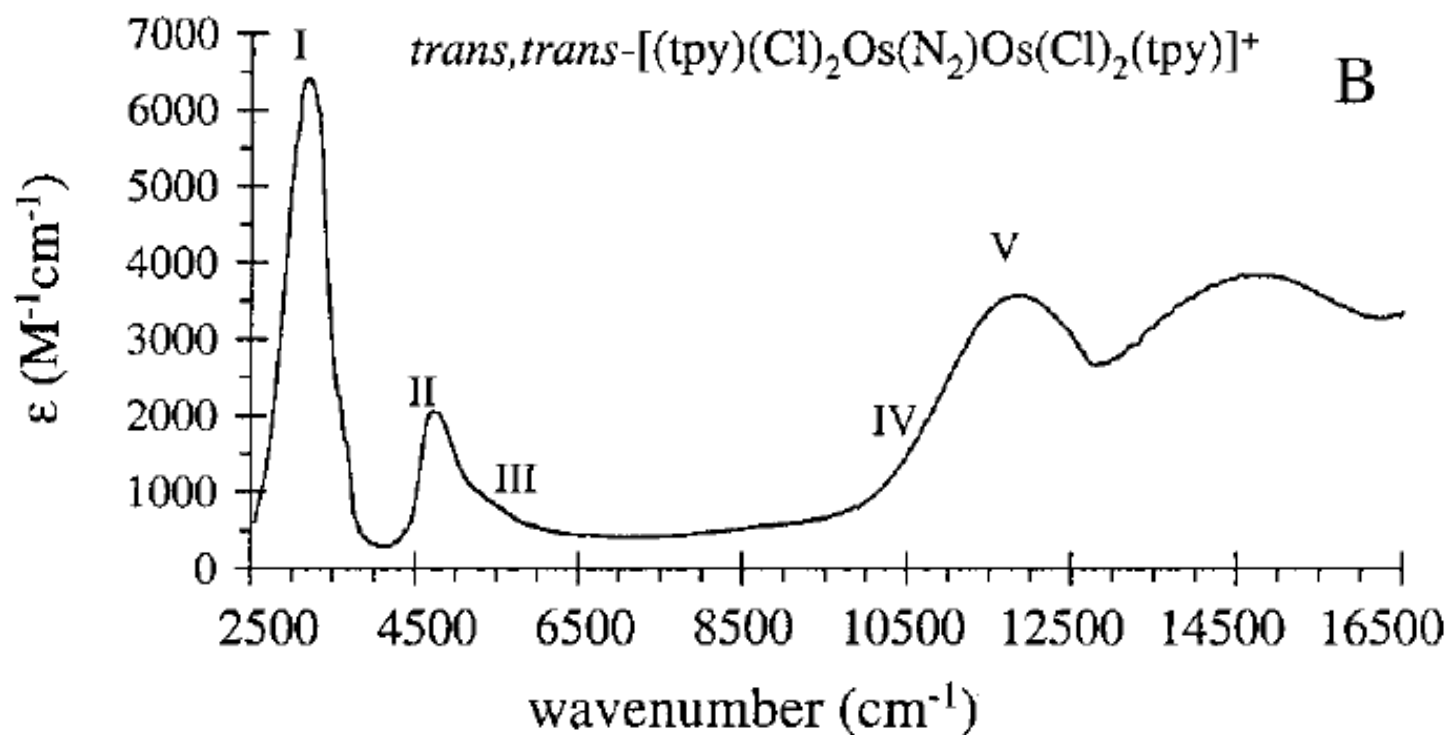
- Bands I (IC-1) and II (IC-2), are called interconfigurational (IC) transitions, assigned to transitions between the Kramer's doublets.
- They are LaPorte forbidden but gain intensity through spin-orbit coupling and M-L mixing.
- IC bands are less commonly observed for Fe(III), $\chi \sim 500 \text{ cm}^{-1}$, or for Ru(III), $\chi \sim 1000 \text{ cm}^{-1}$.



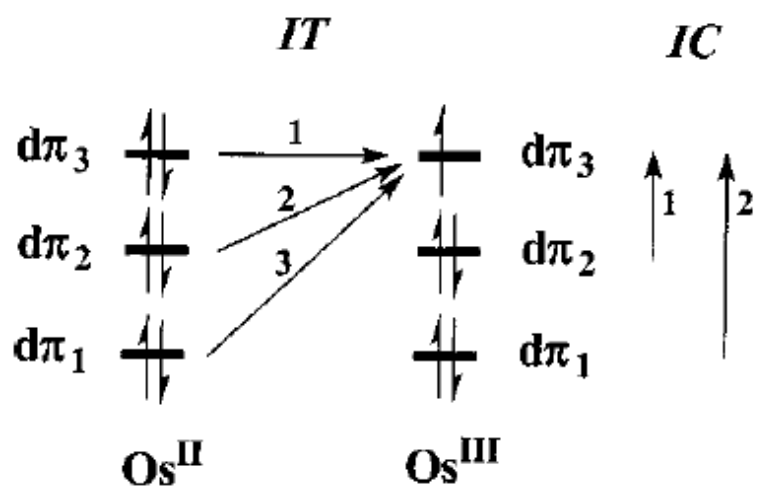


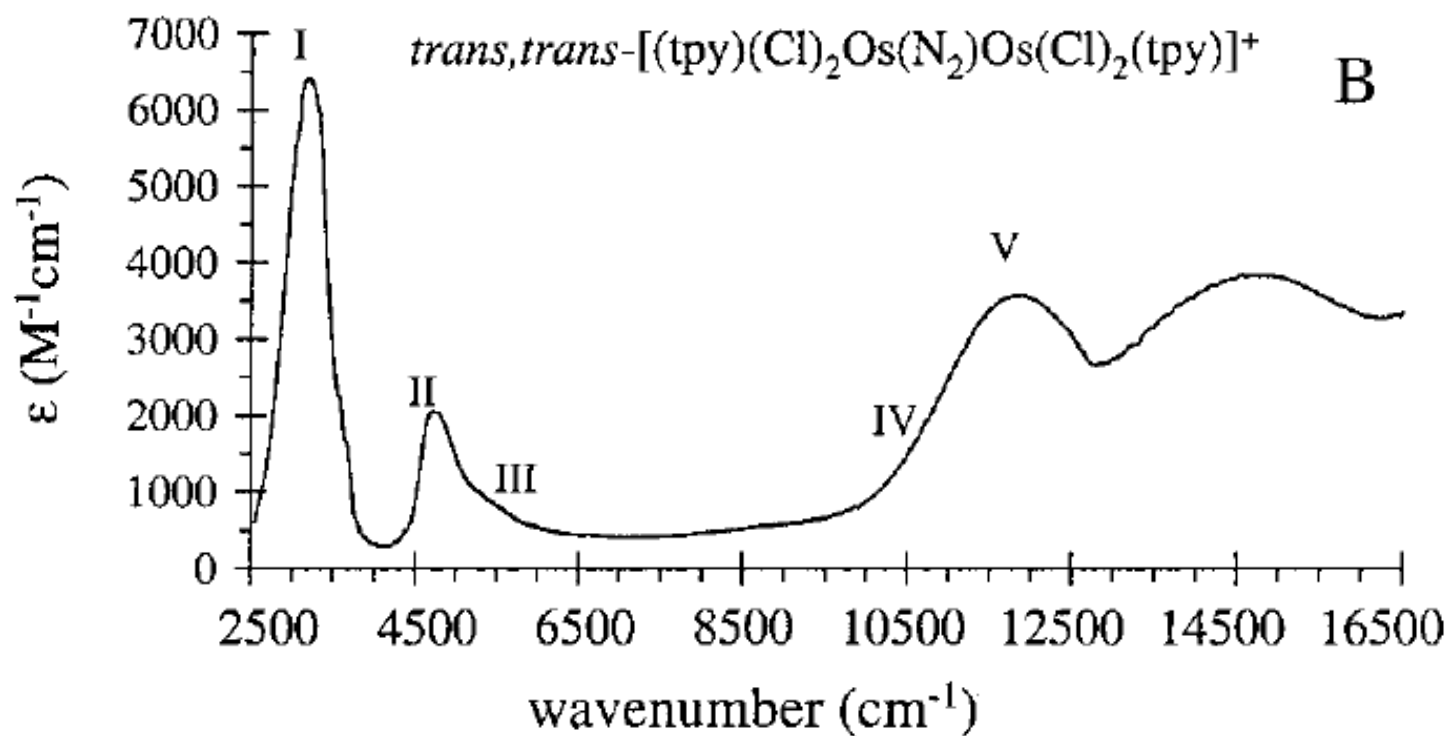
- The remaining three bands (III, IV, V) can be assigned to IT transitions arising from separate electronic excitations across the bridge from the three $d\pi$ orbitals at Os(II) to the hole at Os(III).
- These bands are also narrow but slightly broader than the IC bands, which helps to distinguish them in making band assignments.





- With weaker ligand field splitting in first and second row transition metals the IT transitions typically merge into a single broad overlapping absorption band.
- Transitions IT-2 and IT-3 generate E_2' and E_3' Kramer's doublet configurations at the new Os(III) center.



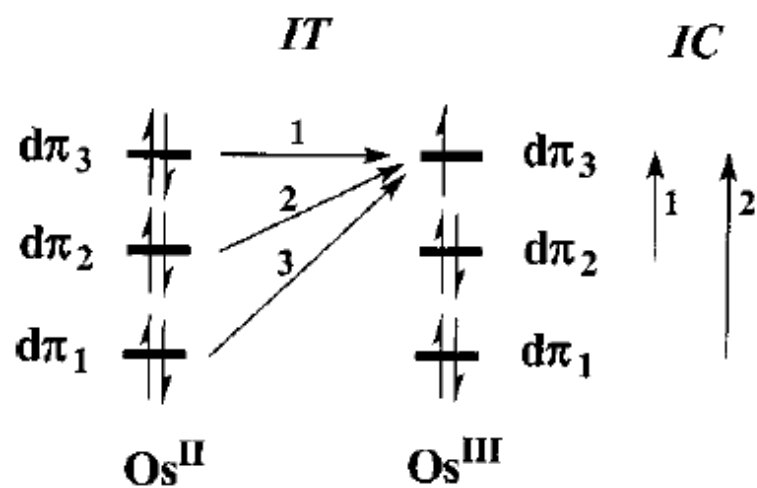


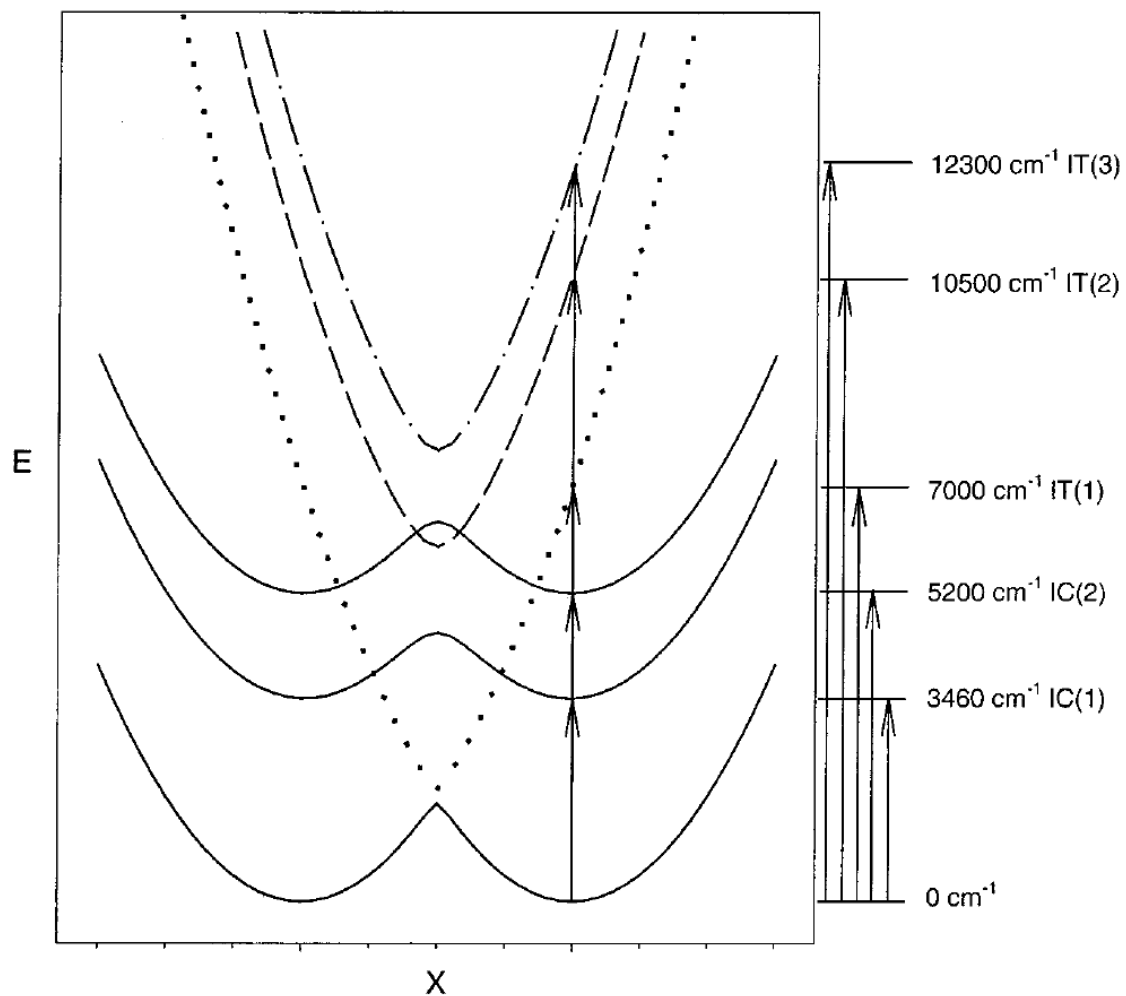
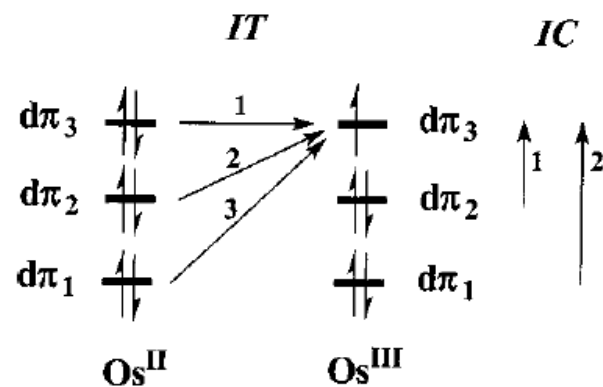
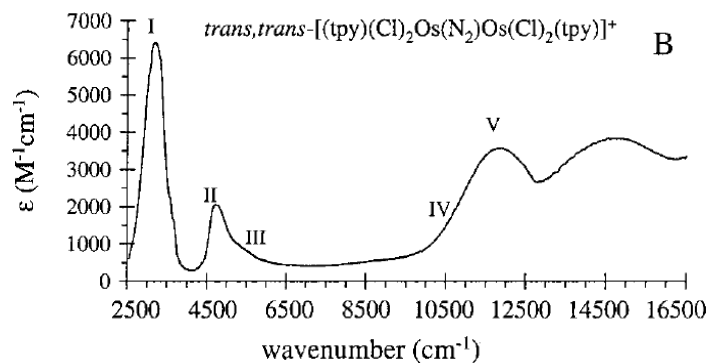
- Assuming the classical limit and a constant λ , the energies of the IC and IT bands are related as

$$E_{IT} (1) = \lambda$$

$$E_{IT} (2) = \Delta G_1^\circ + \lambda \approx E_{IT} (1) + \lambda$$

$$E_{IT} (3) = \Delta G_2^\circ + \lambda \approx E_{IT} (2) + \lambda$$





Energy-coordinate diagrams for E_1 and E_2 calculated using the following eqns.

$$E_1 = \frac{\lambda(2X^2 - 2X + 1)}{2} - \frac{\{[\lambda(2X - 1)]^2 + 4H_{ab}^2\}^{1/2}}{2}$$

$$E_2 = \frac{\lambda(2X^2 - 2X + 1)}{2} + \frac{\{[\lambda(2X - 1)]^2 + 4H_{ab}^2\}^{1/2}}{2}$$

$$\lambda = 7000 \text{ cm}^{-1}$$

$$H_{ab}(1) = 118 \text{ cm}^{-1}$$

The upper two sets of curves were calculated similarly but offsetting by

$$E_{IC}(1) = 3460 \text{ cm}^{-1}$$

$$E_{IC}(2) = 5200 \text{ cm}^{-1}$$

with

$$H_{ab}(2) = 723 \text{ cm}^{-1}$$

$$\text{and } H_{ab}(3) = 595 \text{ cm}^{-1}$$